Electronic Excitation of Rh^I(CO)$_2$ Species on Al$_2$O$_3$ Surfaces: Photodissociation of the Rh^I–CO Bond

Tykhon S. Zubkov, Edward A. Wovchko, and John T. Yates, Jr.*

Surface Science Center, Department of Chemistry, University of Pittsburgh, Pittsburgh, Pennsylvania 15260

Received: January 27, 1999; In Final Form: March 22, 1999

The formation of the Rh^I ion during CO chemisorption on Rh/Al$_2$O$_3$ catalysts has been directly observed using UV–visible spectroscopy. Comparison of infrared and UV–visible spectra indicates that the species Rh^I(CO)$_2$ is produced by a surface oxidation process operating on metallic Rh^0 sites and involving Al–OH groups as oxidizing centers, in agreement with previous postulates.

I. Introduction

One of the important factors controlling chemisorption processes and catalysis on supported metal particles is the structural transformation of the metal as a result of the formation of chemisorption bonds. Reconstruction phenomena can include surface segregation (for alloys)[1] as well as either agglomeration of metal crystallites[2] or their fragmentation. The metal fragmentation can reach an extreme limit through the formation of atomically dispersed metal atoms, as occurs during CO chemisorption on Rh/Al$_2$O$_3$. This extreme metal dispersion process has been studied extensively.[3–22] EXAFS studies by Van't Blik et al.[4] showed that the adsorption of CO drastically changes the local coordination environment of the supported metallic Rh clusters and leads to formation of atomically dispersed Rh sites. It is now generally recognized that these sites are isolated *gem*-dicarbonyl Rh(CO)$_2$ species exhibiting a characteristic IR doublet at around 2100 and 2030 cm^{-1} [4–22] due to symmetric and asymmetric coupling of C–O stretch motions in the isolated species. The formation of isolated Rh(CO)$_2$ was first postulated by Yang and Garland[6] and was supported later by studies of Yates et al.[7–9] and others.

The mechanism of rhodium *gem*-dicarbonyl formation has been deduced through a number of studies. Smith et al.[11,12] and Van't Blik et al.[4] postulated that alumina surface hydroxyl groups were responsible for degradation and oxidation of Rh carbonyl clusters on alumina. Brenner et al.[13,14] performed thermal decomposition of metal carbonyls on Al$_2$O$_3$ and also suggested that reduction of support OH groups was responsible for the formation of oxidized metal centers. Similar conclusions were reached by Solymosi and Pasztor[15,16] who found that an increase in the reduction temperature of a Rh catalyst in a H$_2$ atmosphere led to a decrease of Rh(CO)$_2$ formation, which was attributed to the removal of surface OH species through H$_2$O formation. Direct chemical evidence for the oxidative role of isolated surface OH groups was first provided by IR studies,[5,17] which showed that isolated OH species were consumed during the production of atomically dispersed Rh^I(CO)$_2$ according to the reaction $(1/_x)$Rh^0_x + OH(a) + 2CO(g) → Rh^I(CO)$_2$(a) + $(1/_2)$H$_2$(g). The reaction is reversed by using H$_2$, causing regeneration of isolated OH(a) species and consumption of Rh^I-(CO)$_2$.[5,17]

It is believed that the oxidation state of rhodium in Rh(CO)$_2$ is +1. A number of authors have assigned the rhodium center of the *gem*-dicarbonyl species to Rh^I rather than Rh^0.[4,5,7–22] In much of this work, close analogies between the IR spectrum of Rh^I(CO)$_2$/Al$_2$O$_3$ and the >Rh^I(CO)$_2$ moiety in the organometallic compound [Rh^{I}Cl(CO)$_2$]$_2$ [22] have been employed for indirect assignment of the Rh^I oxidation state. In addition, IR studies of an anchored Rh^I(CO)$_2$ species on SiO$_2$ have also been used in establishing this analogy.[20] More definitive spectroscopic assignments of the Rh^I oxidation state in Rh(CO)$_2$/Al$_2$O$_3$ were based on XPS measurements,[4] NMR measurements,[21] and ESR measurements.[4] Yet even though the Rh^I center should present a distinct electronic spectrum in the UV–vis region, there were only two reports of UV spectral data for Rh^I(CO)$_2$ surface species: one of the studies dealt with a γ-alumina support,[23] the other with a NaY zeolite.[24] The UV absorption maxima the authors reported were not completely identical: 322, 370 nm (reported as 352 nm, which disagrees with the spectrum shown),[23] and 270 and 321 nm.[24] In both cases Rh^I(CO)$_2$ was obtained by direct reduction of Rh^{III} ions with CO.

In this paper we report the results of our spectral studies of the formation of Rh^I(CO)$_2$ from metallic Rh supported on Al$_2$O$_3$ when treated with CO at 300 K. This study produced more definitive UV–vis spectra and provided additional evidence for the production of Rh^I centers. We also propose the band assignment on the basis of recent UV photolysis studies.

II. Experimental Section

Experiments were conducted in a transmission infrared cell described previously.[25] The cell was attached to a stainless steel vacuum/gas handling system. The system was pumped by a turbomolecular pump that maintained a base pressure of 10^{-7} Torr. Gas pressures were measured with an MKS 107A Baratron capacitance manometer.

The 0.5% Rh/Al$_2$O$_3$ sample preparation procedure involved dissolving RhCl$_3$·3H$_2$O (Alfa, 99.9% pure) in ultrapure water (10 mL/g of support), mixing with powdered γ-Al$_2$O$_3$ (Degussa, 101 m^2/g), and ultrasonically dispersing the mixture for 50 min. The slurry was mixed with acetone (EM Science, GR) in a volume ratio of acetone/water = 9/1. The resultant slurry was sprayed with a nitrogen-gas pressured atomizer onto a warmed (330 K) CaF$_2$ disk (sample holder), causing flash evaporation of solvent. One-half side of the disk was exposed to spraying, the other half was shielded. The surface density of the RhCl$_3$/Al$_2$O$_3$ deposit was 1.22 × 10^{-3} g/cm^2. Background spectra were recorded through the clean side of the CaF$_2$ disk. After being sprayed, the disk was mounted in the cell and evacuated at 475

Excitation of $Rh^I(CO)_2$ on Al_2O_3

J. Phys. Chem. B, Vol. 103, No. 25, 1999 **5301**
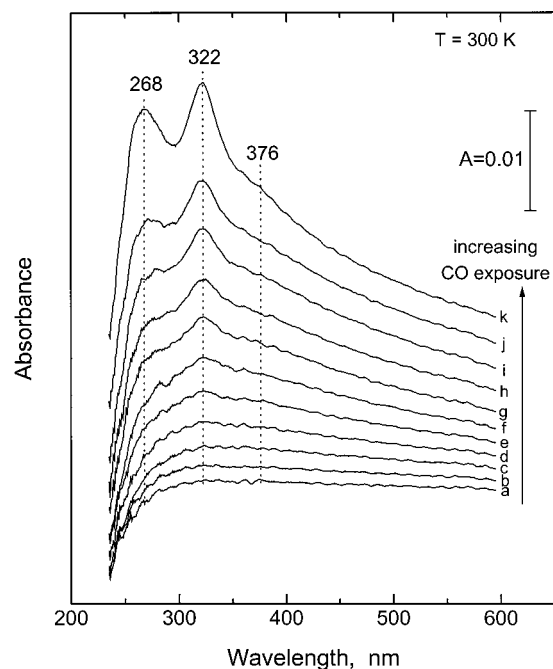
Figure 1. UV spectra of system CO + 0.5% Rh/Al_2O_3 after different exposures to CO (initial spectrum of the sample is subtracted): *(a)* 1 mTorr; (b) 3 mTorr; (c) 10 mTorr; (d) 30 mTorr; (e) 100 mTorr; (f) 300 mTorr; (g) 1 Torr; (h) 3 Torr; (i) 10 Torr; (j) 30 Torr; (k) saturation, 12 h exposure.

Figure 2. IR spectra of system CO + 0.5% Rh/Al_2O_3 after different exposures to CO (initial spectrum of the sample is subtracted): (a) 1 mTorr; (b) 3 mTorr; (c) 7 mTorr; (d) 10 mTorr; (e) 30 mTorr; (f) 100 mTorr; (g) 300 mTorr; (h) 1 Torr; (i) 10 Torr; (j) 30 Torr; (k) saturation, 12 h exposure.

K for ~10 h. Reduction of the sample with H_2 (Matheson 99.9995%) at 475 K was done in four successive exposures at 175, 175, 175, and 200 Torr of H_2 for 15, 15, 15, and 60 min, respectively, with evacuation after each exposure. The reduced sample was evacuated at 475 K for ~10 h, then cooled to 300 K and exposed at 300 K to the appropriate pressure of CO (Airco, 99.999%) in the range 1 mTorr to 30 Torr followed by evacuation for 10 min. The only exception to the procedure occurred in obtaining spectra at saturation coverage. Here, the sample was exposed to 30 Torr of CO for ~12 h and then evacuated for 15 min.

For UV−vis and IR spectral measurements two separate samples were prepared in the same way.

UV−vis measurements were performed with the use of a Perkin-Elmer Lambda 9 UV−vis−NIR spectrophotometer. The spectral slit width was 5 nm. Absorbance spectra were obtained by averaging 10 scans followed by subtraction of the initial absorbance spectrum recorded before any exposure to CO.

Infrared measurements were carried out using a nitrogen-gas-purged Mattson Research series I Fourier transform infrared spectrometer. The spectra were obtained by averaging 1000 scans at 2 cm^{-1} spectral resolution. The ratio of the single-beam transmission spectra of the sample to the initial spectrum (recorded before any exposure to CO) was converted to the absorbance spectrum followed by a baseline correction.

Both UV and IR spectra were smoothed using the Savitzky−Golay method considering 13 data points at a time (Origin 3.5).

III. Results and Discussion

UV−vis spectra for CO chemisorption on 0.5% Rh/Al_2O_3 are shown in Figure 1. As the chemisorption proceeds, bands at 268 and 322 nm develop (features I and II, respectively). At saturation coverage there is an additional weak absorption at 376 nm (feature III).

The development of IR bands corresponding to the above process is shown in Figure 2. The spectra are in agreement with
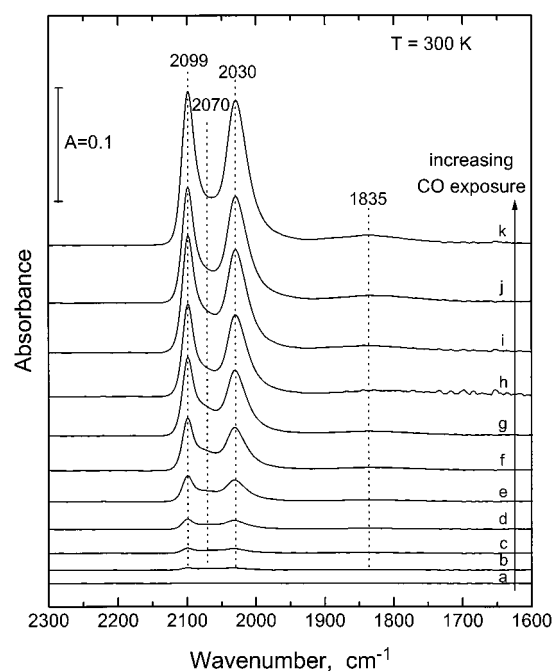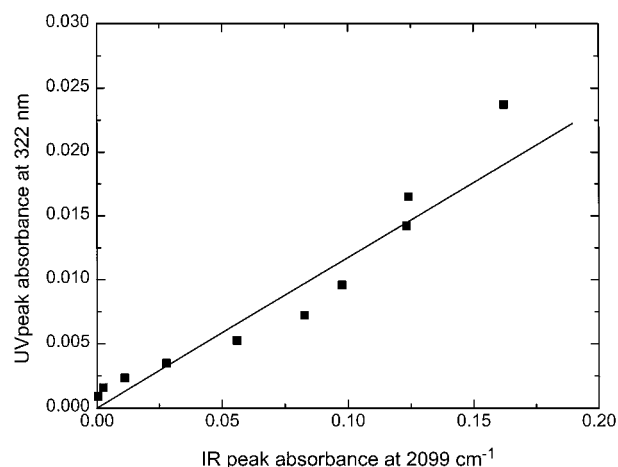
Figure 3. Correlation between UV and IR absorbances of CO + 0.5% Rh/Al_2O_3.

results obtained in previous studies.[5−22] The main infrared features at 2099 and 2030 cm^{-1} are assigned respectively to symmetric and asymmetric C−O stretching vibrations of atomically dispersed *gem*-dicarbonyl, $Rh^I(CO)_2$. The presence of some metallic Rh on the alumina surface is detected from the weak features at 2065−2070 and 1835 cm^{-1}. The broad band around 1835 cm^{-1} is attributed to bridge-bonded CO on Rh crystallites.[26,27] Terminal carbonyl species on metallic Rh sites are observed at ~2070 cm^{-1}. This band is noticeable at the early stages of CO chemisorption but barely seen at higher CO coverages because of overlap with the strong $Rh^I(CO)_2$ doublet.

Figure 3 shows the relationship between the UV absorbance of the 322 nm feature and the IR peak absorbance of the rhodium *gem*-dicarbonyl feature at 2099 cm^{-1}. The correlation is striking, and the nonlinearity is due to uncertainties in the behavior of the background signal in the UV−vis spectra.

TABLE 1: Rh(CO)$_2$ Electronic Absorption Spectral Data

	UV spectral features			
species	I	II	III	ref
[Rh^I(CO)$_2$Cl]$_2$	260	318	(365, 370)^a	28
[Rh^I(CO)$_2$Cl$_2$]$^-$	270	336		29
[Rh^I(CO)$_2$Br$_2$]$^-$	275	337		29
[Rh^I(CO)$_2$(PhNH$_2$)X]^b	265	335		30
[Rh^I(CO)$_2$(pyO)X]^b	271	327		31
Rh^I(CO)$_2$/Al$_2$O$_3$	(~270)^c	322	370^d	23
Rh^I(CO)$_2$/NaY	270	321	(~370−380)^c	24
Rh^I(CO)$_2$/Al$_2$O$_3$	268	322	377	this work
[Rh^{III}$_2$(CO)$_4$(SO$_4$)$_2$(μ-Cl)(μ-5-dppn)]Cl^e	286	316	350	32
Rh^{II}(CO)$_2$− and Rh^0(CO)$_2$− species	no data			

^{a} Not observed in CH$_2$Cl$_2$ solution but observed in diethyl ether and THF. ^{b} X = Cl, Br; pyO = pyridine-N-oxide. ^{c} Not reported, but present on the spectra shown ^{d} Reported incorrectly as 352 nm, which does not agree with experimental spectrum shown. ^{e} 5-dppn = 6,7-dihydro-1,4-di(2′-pyridyl)-5H-cyclopenta{d}pyridazine.
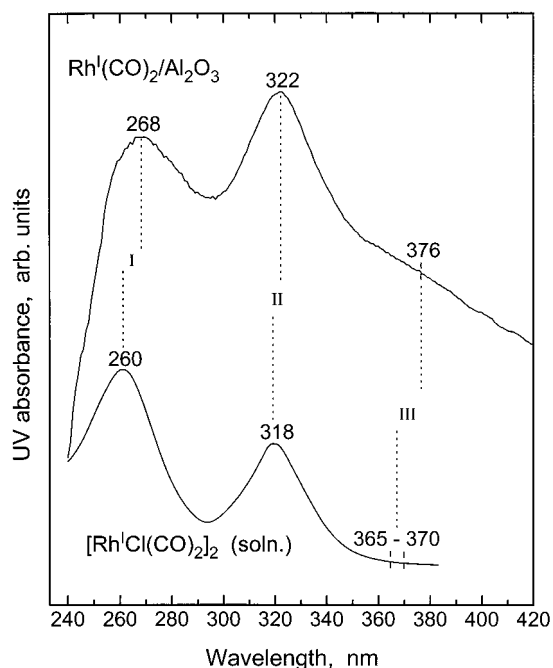

Figure 4. UV spectra of Rh^I(CO)$_2$/Al$_2$O$_3$ and [Rh^{I}Cl(CO)$_2$]$_2$ (solution).[28]

The UV−vis spectra obtained in this work are compared to UV−vis spectra for solutions of Rh(I) *cis*-dicarbonyl complexes with square-planar ligand environment. Figure 4 illustrates the similarity between the spectra of Rh^I(CO)$_2$/Al$_2$O$_3$ and the chlorobridged dimer [Rh^{I}Cl(CO)$_2$]$_2$ (CH$_2$Cl$_2$ solution).[28] The low-intensity band at 376 nm in the Rh^I(CO)$_2$/Al$_2$O$_3$ spectrum does not seem to have a counterpart in the [Rh^{I}Cl(CO)$_2$]$_2$ spectrum measured in CH$_2$Cl$_2$ solvent. However, Epstein et al.[28] showed that magnetic circular dichroism (MCD) spectra of the chlorocarbonyl species in CH$_2$Cl$_2$ solution do contain a weak absorption band at 360 nm, and the 360 nm band of [Rh^{I}Cl-(CO)$_2$]$_2$ was also observed in THF (370 nm) and diethyl ether (365 nm) solutions.

Table 1 gives a comparison of absorption peak positions for different square-planar Rh(I) dicarbonyl complexes.[28−31] These data show a close correspondence between electronic spectral properties of the surface species and the Rh^I center in the metal carbonyls.

Table 1 also contains the aforementioned UV data for supported Rh dicarbonyl species.[23,24] Comparison of our results with them reveals striking correspondence. It is easy to see that both series of electronic transitions reported earlier are parts of one spectrum. In fact, one can see the missing bands (~270 nm in ref 23 and ~370 nm shoulder in ref 24) in the spectra presented in those papers, but the authors did not mention and comment on them.

Unfortunately, we were unable to show a comprehensive comparison of the UV spectra for rhodium *cis*-dicarbonyl species with a different oxidation state of rhodium because there are very few reports about formation of rhodium dicarbonyls with a rhodium oxidation state other than +1.[32−38] The only exception is the UV spectrum of Rh^{III}(CO)$_2$ [32] (the only example of the formation of Rh^{III} dicarbonyl). Data in Table 1 show that the electronic spectrum of this species differs somewhat from the spectra for Rh^I dicarbonyls. No UV data are available for Rh-(CO)$_2$ species with an Rh oxidation state of +2 or 0. Rare reports about Rh^{II} *gem*-dicarbonyls[33,34] and Rh^0 *gem*-dicarbonyls[35] showed that these species exist as dimers, giving IR patterns different from those observed in our case. These patterns differ even more if CO molecules attach as bridging species on Rh(II or 0) dimer.[36−38]

The results presented here are conclusive in assigning the Rh(CO)$_2$/Al$_2$O$_3$ species as involving the Rh^I oxidation state. Coupling of Rh^I to oxygen anion(s) in the Al$_2$O$_3$ surface must occur in analogy to the Rh−X bonding in compounds such as [Rh^{I}Cl(CO)$_2$]$_2$.

Some details regarding the band assignment may be mentioned. According to Epstein et al. [28] for Rh complexes of C_{2v} symmetry, the two lowest energy bands are the triplet and singlet components of d$_{z^2}$ → L$_\pi$ excitation. Therefore, assuming one-electron excitation, feature II can be assigned to the spin-allowed component (singlet → singlet) of the transition 2a$_1$(z^2) → 2b$_1$ and feature III to the spin-forbidden component (singlet → triplet) of the same transition, which can take place in the presence of spin−orbit coupling when spin-multiplicity selection rules break down. The high-energy band (feature I) can be assigned to the spin-allowed transition a$_2$(yz), 1b$_1$(xz) → 2b$_1$. These transitions are summarized in Figure 5a.

According to this band assignment, UV photoexcitation of an electron into the 2b$_1$ molecular orbital must strengthen the Rh−C bond, since the 2b$_1$ orbital is metal−ligand bonding in nature. However, numerous studies[39−44] have shown that UV irradiation of Rh^I(CO)$_2$/Al$_2$O$_3$ causes the photodesorption of CO. Loss of a CO ligand is also readily observed during the ultraviolet photolysis of organometallic transition metal carbonyls as well.[45−49] This indicates that electron transfer from filled d orbitals to the b$_2$(xy) metal−ligand antibonding molecular orbital takes place, causing Rh−CO bond-breaking. The precise energies of the 2b$_1$ and b$_2$(xy) molecular orbitals for Rh^I(CO)$_2$/Al$_2$O$_3$ are unknown. Therefore, we cannot distinguish between
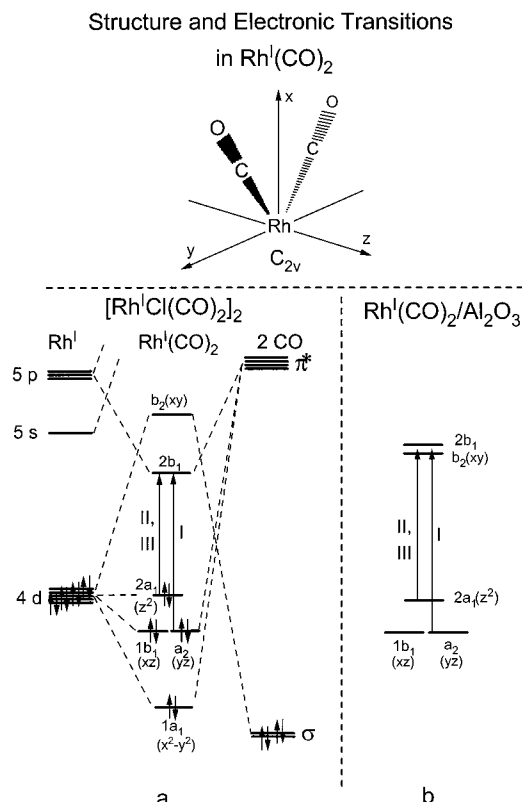
Figure 5. Molecular orbital diagram for the Rh^I(CO)$_2$ complexes of C_{2v} symmetry, showing the assignment of the observed electronic transitions: (a) [Rh^{I}Cl(CO)$_2$]$_2$ (according to ref 28); (b) Rh^I(CO)$_2$/Al$_2$O$_3$.

excitations to 2b$_1$ or b$_2$ MO's. The observed UV absorption in Figure 4 may involve excitation to either orbital as shown in Figure 5b.

Spectroscopic studies of the wavelength-dependent photoexcitation of Rh^I(CO)$_2$/Al$_2$O$_3$ are discussed in greater detail in an earlier publication.[50]

References and Notes

(1) Bowman, R.; Sachtler, W. M. H. *J. Catal.* **1970**, *19*, 127.

(2) *Metal clusters in catalysis*; Gates, B. C., Guczi, L., Knözinger, H., Eds.; Elsevier: New York, 1986.

(3) Gates, B. C. *Chem. Rev.* **1995**, *95*, 54.

(4) Van't Blik, H. F. J.; Van Zon, J. B. A. D.; Huizinga, T.; Vis, J. C.; Koningsberger, D. C.; Prins, R. *J. Am. Chem. Soc.* **1985**, *107*, 3139.

(5) Basu, P.; Panayotov, D.; Yates, J. T., Jr. *J. Phys. Chem.* **1987**, *91*, 3133.

(6) Yang, A. C.; Garland, C. W. *J. Phys. Chem.* **1957**, *61*, 1504.

(7) Yates, J. T., Jr.; Duncan, T. M.; Worley, S. D.; Vaughan, R. W. *J. Chem. Phys.* **1979**, *70*, 1219.

(8) Yates, J. T., Jr.; Duncan, T. M.; Vaughan, R. W. *J. Chem. Phys.* **1979**, *71*, 3908.

(9) Cavanagh, R. R.; Yates, J. T., Jr. *J. Chem. Phys.* **1981**, *74*, 4150.

(10) Rice, C. A.; Worley, S. D.; Curtis, C. W.; Guin, J. A.; Tarrer, A. R. *J. Chem. Phys.* **1981**, *74*, 6487.

(11) Smith, A. K.; Hugues, F.; Theolier, A.; Basset, J. M.; Ugo, R.; Zanderighi, G. M.; Bilhou, J. L.; Bilhou-Bougnal, V.; Graydon, W. F. *Inorg. Chem.* **1979**, *18* (11), 3104.

(12) Bilhou, J. L.; Bilhou-Bougnal, V.; Graydon, W. F.; Basset, J. M.; Smith, A. K.; Zanderighi, G. M.; Ugo, R. *J. Organomet. Chem.* **1978**, *153*, 73.

(13) Brenner, A.; Hucul, D. A. *J. Catal.* **1980**, *61*, 216.

(14) Hucul, D. A.; Brenner, A. *J. Phys. Chem.* **1981**, *85*, 496.

(15) Solymosi, F.; Pasztor, M. *J. Phys. Chem.* **1985**, *89*, 4789.

(16) Solymosi, F.; Pasztor, M. *J. Phys. Chem.* **1986**, *90*, 5312.

(17) Basu, P.; Panayotov, D.; Yates, J. T., Jr. *J. Am. Chem. Soc.* **1988**, *110*, 2074.

(18) Primet, M. *J. Chem. Soc., Faraday Trans. 1* **1978**, *74*, 2570.

(19) Andersson, S. L. T.; Scurrell, M. S. *J. Catal.* **1979**, *59*, 340.

(20) Knözinger, H.; Thornton, E. W.; Wolf, M. *J. Chem. Soc., Faraday Trans. 1* **1979**, *75*, 1888.

(21) Robbins, J. L. *J. Phys. Chem.* **1986**, *90*, 3381.

(22) Yates, J. T., Jr.; Kolasinski, K. *J. Chem. Phys.* **1983**, *79*, 1026.

(23) Krzywicki, A.; Marczewski, M. *J. Mol. Catal.* **1979**, *6*, 431.

(24) Primet, M.; Garbowski, E. *Chem. Phys. Lett.* **1980**, *72* (3), 472.

(25) Beebe, T. P.; Gelin, P.; Yates, J. T., Jr. *Surf. Sci.* **1984**, *148*, 526.

(26) Dubois, L. H.; Somorjai, G. A. *Surf. Sci.* **1980**, *91*, 514.

(27) Leung, L.-W. H.; He, J.-W.; Goodman, D. W. *J. Chem. Phys.* **1990**, *93*, 8328.

(28) Epstein, R. A.; Geoffroy, G. L.; Keeney, M. E.; Mason, W. R. *Inorg. Chem.* **1979**, *18* (2), 478.

(29) Geoffroy, G. L.; Isci, H.; Litrenti, J.; Mason, W. R. *Inorg. Chem.* **1977**, *16* (8), 1950.

(30) Hall, P. S.; Jackson, G. E.; Moss, J. R.; Thorton, D. A. *Spectroscopy (Amsterdam)* **1993**, *11*, 9.

(31) Hall, P. S.; Jackson, G. E.; Moss, J. R.; Thorton, D. A. *J. Alloys Compd.* **1993**, *197*, 69.

(32) Esmadi, F.; Al-Hamid, A. *Transition Met. Chem.* **1994**, *19*, 571.

(33) Connelly, N. G.; Daykin, H.; Demidowicz, Z. *J. Chem. Soc., Dalton. Trans.* **1978**, 1532.

(34) Bitterwolf, T. E.; Spink, W. C.; Rausch, M. D. *J. Organomet. Chem.* **1989**, *363*, 189.

(35) Nazmutdinova, V. N.; Chirkova, L. P.; Mukhamadeeva, R. N.; Plyamovatyi, A. Kh.; Gainullin, R. M.; Pudovik, M. A.; Polovnyak, V. K.; Pudovik, A. N. *Russ. J. Gen. Chem.* **1994**, *64* (10), 1442.

(36) Matthews, R. C.; Howell, D. K.; Peng, W.-J.; Train, S. G.; Treleaven, W. D.; Stanley, G. G. *Angew. Chem., Int. Ed. Engl.* **1996**, *35*, 2253.

(37) Evans, D.; Yagupsky, G.; Wilkinson, G. *J. Chem. Soc. A* **1968**, Part III, 2660.

(38) Gregorio, G.; Pregaglia, G.; Ugo, R. *Inorg. Chim. Acta* **1969**, *3* (1), 89.

(39) Ballinger, T. H.; Yates, J. T., Jr. *J. Am. Chem. Soc.* **1992**, *114*, 10074.

(40) Ballinger, T. H.; Yates, J. T., Jr. *J. Phys. Chem.* **1992**, *96*, 9979.

(41) Wong, J. C. S.; Yates, J. T., Jr. *J. Am. Chem. Soc.* **1994**, *116*, 1610.

(42) Wong, J. C. S.; Yates, J. T., Jr. *J. Phys. Chem.* **1995**, *99*, 12640.

(43) Wovchko, E. A.; Yates, J. T., Jr. *J. Am. Chem. Soc.* **1995**, *117*, 12557.

(44) Wovchko, E. A.; Yates, J. T., Jr. *J. Am. Chem. Soc.* **1996**, *118*, 10250.

(45) Wrighton, M. *Chem. Rev.* **1974**, *74*, 401.

(46) Wasserman, E. P.; Moore, C. B.; Bergman, R. G. *Science* **1992**, *255*, 315.

(47) Schultz, R. H.; Bengali, A. A.; Tauber, M. J.; Weiller, B. H.; Wasserman, E. P.; Kyle, K. R.; Moore, C. B.; Bergman, R. G. *J. Am. Chem. Soc.* **1994**, *116*, 7369.

(48) Dougherty, T. P.; Grubbs, W. T.; Heilweil, E. J. *J. Phys. Chem.* **1994**, *98*, 9396.

(49) Lees, A. J.; Purwoko, A. A. *Coord. Chem. Rev.* **1994**, *132*, 155.

(50) Wovchko, E. A.; Zubkov, T. S.; Yates, J. T., Jr. *J. Phys. Chem. B* **1998**, *102*, 10535.